Simulations of vortex generators

By P. Koumoutsakos

1. Motivation and background

We are interested in the study, via direct numerical simulations, of active vortex generators. Vortex generators may be used to modify the inner part of the boundary layer or to control separation thus enhancing the performance and maneuverability of aerodynamic configurations. We consider generators that consist of a surface cavity elongated in the stream direction and partially covered with a moving lid that at rest lies flush with the boundary. Streamwise vorticity is generated and ejected due to the oscillatory motion of the lid. The present simulations complement relevant experimental investigations of active vortex generators at NASA Ames and Stanford University (Saddoughi ,1994, and Jacobson and Reynolds, 1993). Jacobson and Reynolds (1993) used a piezoelectric device in water, allowing for small amplitude high frequency oscillations. They placed the lid asymmetrically on the cavity and observed a strong outward velocity at the small gap of the cavity. Saddoughi used a larger mechanically driven device in air to investigate this flow and he observed a jet emerging from the wide gap of the configuration, contrary to the findings of Jacobson and Reynolds.

Our task is to simulate the flows generated by these devices and to conduct a parametric study that would help us elucidate the physical mechanisms present

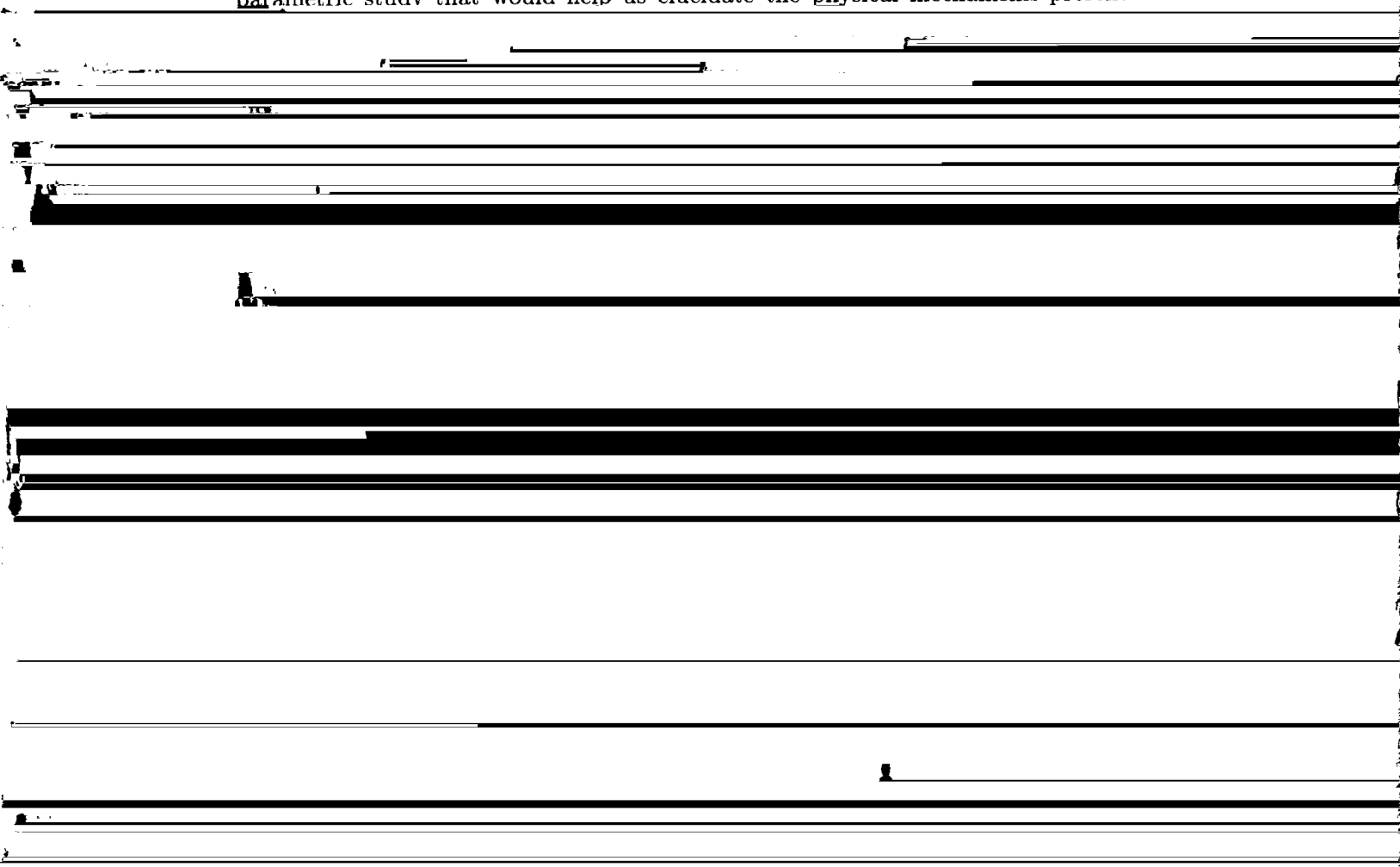

ulating flows around complex configurations undergoing arbitrary motions. Here

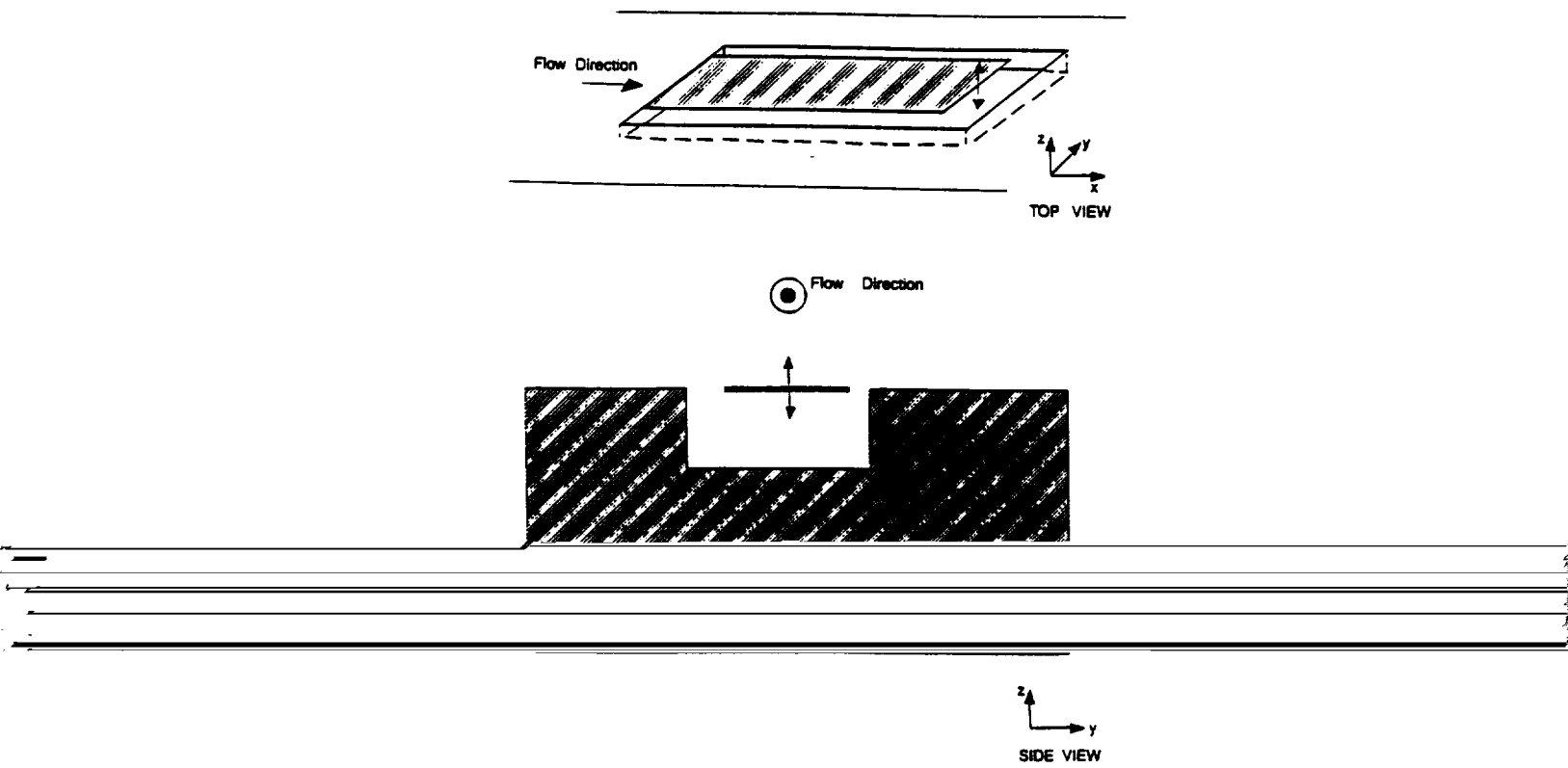

FIGURE 1. Definition sketch.

where $\mathbf{u}(\mathbf{x},t)$ is the velocity, $\boldsymbol{\omega} = \omega \hat{\mathbf{e}_z} = \nabla \times \mathbf{u}$ the vorticity and ν denotes the kinematic viscosity . Using the definition of the vorticity and the continuity ($\nabla \cdot \mathbf{u} = 0$) it can be shown that $\mathbf{u}$ is related to $\boldsymbol{\omega}$ by a Poisson equation

$$\nabla^2 \mathbf{u} = -\nabla \times \boldsymbol{\omega} \tag{2}$$

The vorticity equation (Eq. 1) may be expressed in a Lagrangian formulation by solving for the vorticity carrying fluid elements ($\mathbf{x_a}$) based on the following set of equations:

$$\begin{aligned} \frac{d\mathbf{x_a}}{dt} &= \mathbf{u}(\mathbf{x_a},t) \\ \frac{\mathrm{d}\omega}{\mathrm{d}t} &= \nu \nabla^2 \omega \end{aligned} \tag{3}$$

For flow around a non-rotating body, moving with velocity $\mathbf{U_b}(t)$, the velocity of the fluid ($\mathbf{u}$) on the surface of the body ($\mathbf{x}_s$) is equal to the velocity of the body: $\mathbf{u}(\mathbf{x}_s,t) = \mathbf{U_b}(\mathbf{t})$ At infinity we have: $\mathbf{u}(\mathbf{x}) \rightarrow \mathbf{U}_\infty$ as $|\mathbf{x}| \rightarrow \infty$ where $\mathbf{U}_\infty$ is the free stream velocity.

2.2 Particle (vortex) methods

The present numerical method is based on the discretization of the above equations in a Lagrangian frame using particle (vortex) methods. The vorticity field

is considered as a discrete sum of the individual vorticity fields of the computational particles, having core radius ϵ, strength $\Gamma(t)$, and an individual distribution of vorticity determined by the function η_ϵ, so that:

$$\omega(\mathbf{x},t) = \sum_{n=1}^{N} \Gamma_n(t)\, \eta_\epsilon(\mathbf{x} - \mathbf{x}_n(t)) \tag{4}$$

In the context of vortex methods the right-hand side of Eq. 3 is replaced by integral operators. The velocity field may be determined from the vorticity field using the Green's function formulation for the solution of Poisson's equation (Eq. 2).

$$\mathbf{u} = = -\frac{1}{2\pi}\int \mathbf{K}(\mathbf{x} - \mathbf{y}) \times \boldsymbol{\omega}\, d\mathbf{y} + \mathbf{U}_0(\mathbf{x},t) \tag{5}$$

where $\mathbf{U}_0(\mathbf{x},t)$ accounts for the presence of the body and $\mathbf{U}_\infty$, and $\mathbf{K}(\mathbf{z}) = \mathbf{z}/|\mathbf{z}|^2$. The use of the Biot-Savart law to compute the velocity field guarantees the enforcement of the boundary condition at infinity.

The Laplacian operator may be approximated by an integral operator (Mas-Gallic, 1987) as well:

$$\nabla^2\omega \approx \int G_\epsilon(|\mathbf{x} - \mathbf{y}|)\, [\omega(\mathbf{x}) - \omega(\mathbf{y})]\, d\mathbf{y} \tag{6}$$

These integrals are discretized using a quadrature having as quadrature points the locations of the particles. Fast multipole algorithms with a computational cost scaling as $\mathcal{O}(N)$ (Greengard and Rohklin, 1987) have been efficiently implemented, allowing for high resolution simulations using a few millions of particles (grid points).

The no-slip boundary condition is enforced by formulating the physical mecha-

2.3 Fractional step algorithm - boundary conditions

A fractional step algorithm is implemented that accommodates the enforcement of the no-slip boundary condition. Let us assume that at the n-th time step (corresponding to time $t - \delta t$) the vorticity field has been computed (respecting the no-slip boundary condition) and we seek to advance the solution to the next time step (time t). The following two-step procedure is implemented:

•Step 1 (kinematics-no through flow):

Particles are advanced via the Biot-Savart law and their strength is modified based on the scheme of particle strength exchange. In order to account for the presence of the body the no-through flow needs to be enforced. This is accomplished by distributing vortex sheets on the surface of the bodies. For a doubly connected domain as that shown in Fig. 1b the potential flow problem is solved using the following set of equations:

$$\int_{-L/2}^{L/2} \frac{\kappa(\boldsymbol{\xi})}{\mathbf{x}_p - \boldsymbol{\xi}} d\boldsymbol{\xi} + \int_{-\infty}^{\infty} \gamma_w(\boldsymbol{\zeta}) \frac{\partial}{\partial s(\mathbf{x}_p)} Log|\boldsymbol{\zeta} - \mathbf{x}_p| \, d\boldsymbol{\zeta} = \mathbf{u}_n(\mathbf{x}_p) \qquad 8a$$

$$\int_{-L/2}^{L/2} \kappa(\xi, t) d\xi = -\nu \int_0^t \int_{-L/2}^{L/2} \frac{\partial \omega(\mathbf{x}_p, T)}{\partial n(\mathbf{x}_p)} d\mathbf{x}_p \, dT \qquad (8b)$$

$$\int_{-L/2}^{L/2} \kappa(\boldsymbol{\xi}) \frac{\partial}{\partial n(\boldsymbol{\zeta})} Log|\boldsymbol{\zeta} - \boldsymbol{\xi}| d\boldsymbol{\xi} + \int_{-\infty}^{\infty} \gamma_w(\boldsymbol{\zeta}') \frac{\partial}{\partial n(\boldsymbol{\zeta})} Log|\boldsymbol{\zeta} - \boldsymbol{\zeta}'| \, d\boldsymbol{\zeta}' = \mathbf{u}_t(\boldsymbol{\zeta}) \quad (8c)$$

where $\kappa(\boldsymbol{\xi}), \mathbf{x}_p$ and $\gamma_w(\boldsymbol{\zeta}), \boldsymbol{\zeta}$ denote vortex sheets and location of points on the surface of the plate and the cavity respectively.

The above set of equations, when discretized using a panel method, results in a well posed system of equations (Koumoutsakos and Leonard, 1995), which can be solved iteratively. Note that Eq. 8b guarantees the solvability of the equations and the uniqueness of the pressure distribution on the surface of the bodies.

•Step 2 (dynamics - no slip):

The no-slip boundary conditions are enforced in this stage by a vorticity (not particle) creation algorithm. The vortex sheet that is distributed on the surface of the body enters the fluid, thus generating a vorticity flux at the surface of the body. This vorticity flux accounts for the modification of the strength of the particles so as to enforce the no-slip boundary condition. Algorithmically, in this step, the diffusion equation is solved on a Lagrangian frame with Neuman boundary conditions. Please see Koumoutsakos *et al.* (1994) for further details.

2.4 Results

A series of simulations have been carried out to determine the important parameters of the flow. It has been speculated that the parameters of the flow such as the frequency of oscillation (f), the gap diameter (d_s, d_l for the small and the large

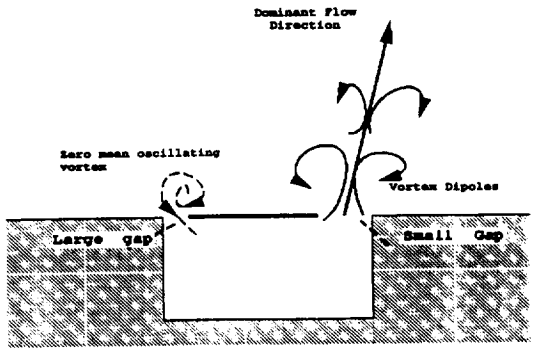

FIGURE 2. Sketch of flow type I.

gap respectively), and the viscosity of the flow may be combined so as to produce a coefficient, called the *Stokes number*:

$$St^{s,l} = \sqrt{\frac{2\pi f d_{s,l}^2}{\nu}}$$

to characterize the different physical phenomena of the flow. We have performed a series of computations by varying the above parameters of the flow along with the amplitude of the oscillations in an attempt to match the respective experimental cases. The simulations have shown a dramatic difference in the flow behavior for various parameters of the configuration. In the following we present the types of flows that are being observed (and described below) computationally and experimentally, along with the respective Stokes numbers.

Large Gap	Small Gap	Flow Type
12.600(Exp.)	2.960 (Exp.)	I
34.010	14.680	I
53.238	14.589	I
4.652 (Exp.)	0.930 (Exp.)	II
15.597	1.794	II
13.870	3.381	II
46.515	9.744	II

In what we call *flow type I*, a positive (inducing an outward velocity) vortex dipole establishes itself in the small gap region just outside the cavity. The pair is produced by the downward motion of the plate. It is continuously fed by the downward motion of the oscillation cycle in such a way as to overcome its erosion by diffusion. The self induced velocity of the dipole, on the other hand, is balanced by the upward motion of the plate, thus establishing a quasi-steady vorticity distribution at the small gap of the configuration. On the large gap side, the distance of the plate from the cavity walls is such that no strong vorticity is being ejected from the cavity walls. The vorticity that is produced at the tip of the plate has a zero mean strength, and diffusion acts to reduce its strength rapidly. Hence as the plate is oscillating no

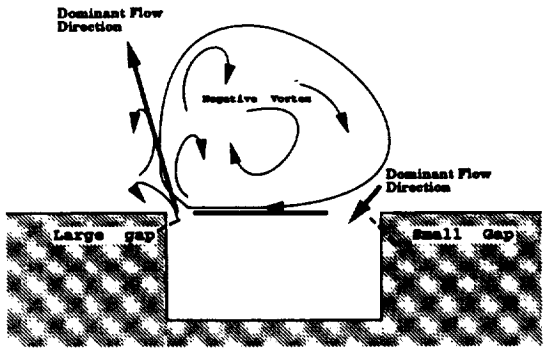

FIGURE 3. Sketch of flow type II.

dominant vortical features are established at this end of the lid. As we reduce the frequency of oscillations, we may observe that dipoles are being ejected from the small gap of the cavity at the downward motion of the plate, while a new pair is being formed at the small gap. However,the dipoles that emerge from the gaps are quickly eroded by diffusion and do not significantly alter the character of the flow.

A strikingly different pattern is observed in *flow type II.* In this configuration, the lid is relatively closer to both edges of the cavity and the amplitude of oscillations is about an order of magnitude in absolute value larger than the previous cases. Hence vortex dipoles are being formed on both gaps of the cavity. The stronger pairs are initially formed in the area of the small gap. Due to the low frequency of the plate oscillations, the upwash motion of the plate does not overcome the self-induced velocity of the vortical pairs and vorticity is ejected from both gaps. However, as the dipoles that are being formed at the large side of the cavity are more asymmetric, with the clockwise vorticity being more dominant, their path arches towards the cavity lid. This establishes, at later times, a large clockwise vortical region over the cavity. This vortex in turn, further modifies the behavior of the flow as it induces an additional downwash velocity on the small side of the gap. The effect of this clockwise (negative) vortex on the flow at the small gap side is twofold: (a) It diverts the positive vortex that is formed at the tip of the lid during the downward motion of the plate in a direction parallel to the lid and (b) it induces an additional downwash velocity. Thus the dipole strength is progressively reduced at the small gap, resulting in a blockage of the vorticity production and fluid ejection from the small gap. The final configuration with the large negative vortex over the cavity lid appears to be stable, thus establishing a flow field with a main jet of fluid emanating form the large gap side of the cavity.

The above described mechanisms may offer an initial tentative 'two-dimensional explanation' to the different behavior exhibited by the flow in the experiments of Jacobson and Reynolds (1995) and Saddoughi (1994). A more systematic study (see below) of the configuration is in order while future three-dimensional simulations would reveal the full mechanism of vorticity generation and flow ejection from the gaps observed in the experiments.

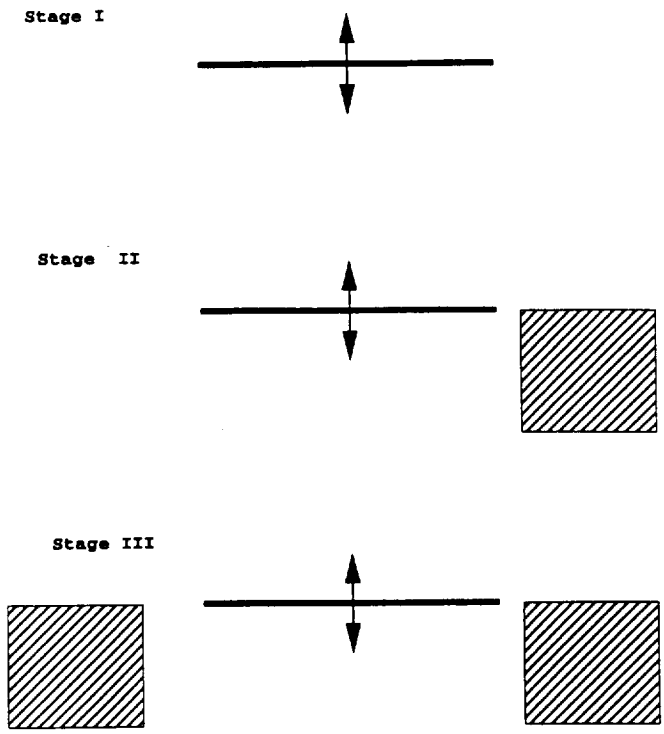

FIGURE 4. Proposed simulated configurations.

3. Conclusions and future work

We have presented simulation of flows past complex configurations undergoing arbitrary motions using a Lagrangian computational scheme based on high resolution viscous vortex methods. The results of these computations attempt to elucidate some of the intricate behavior that has been observed in related experimental works on flows past active vortex generators.

In order to investigate further the mechanisms of vorticity generation and the observed flow patterns, we are in the process of conducting further detailed simulations. More specifically (Fig. 4) each stage of our study would attempt to isolate and examine a different aspect of vorticity generation and destruction which appear in these vortex generators.

(i) In the first stage we are in the process of conducting simulations of a free oscillating plate. This study would help us establish the generation of vorticity at the cavity lids as well as demonstrate the effect of the frequency of oscillation in the generation of vorticity and the interplay of vorticity generation and destruction due to the plate oscillation and diffusion. A theoretical analysis would be conducted to examine the limit of very high frequency oscillations.

(ii)In the second stage of our study, we would examine the interaction of the plate with a corner. This study would help us understand the vorticity formation

at both gaps of the full configuration. By varying the distance of the plate from the cavity we would be able to determine distances as well as frequencies and amplitudes of oscillation for which a vortex dipole is being formed, and we would be able to determine when the effects of the cavity is negligible.

(iii) In the third stage, the full configuration would be examined in a more careful and systematic manner based on our gained insight from the studies of the more simplified configurations.

We are also in the process of developing three-dimensional codes (Koumoutsakos, 1995) for the study of the full configuration that would elucidate the three-dimensional aspects of the flow.

Acknowledgments

I wish to acknowledge many insightful discussions with Dr. Nagi N. Mansour.

REFERENCES

BEALE, J. T. 1986 On the accuracy of vortex methods at large times. *Proc. Workshop on Comp. Fluid Dyn. and React. Gas Flows.* IMA, Univ. of Minnesota.

GREENGARD, L. & ROHKLIN, V. 1987 A fast algorithm for particle simulations. *J. Comp. Phys.* **73,** 325-348.

JACOBSON, S. & REYNOLDS, W. C. 1993 Active boundary layer control using flush-mounted surface actuators. *Bulletin of the American Physical Society.* **96,** 2197.

KOUMOUTSAKOS, P. & LEONARD, A. 1995 High Resolution simulations of the flow past an impulsively started cylinder. *J. Fluid Mech.* **96,** 1-32.

KOUMOUTSAKOS, P., LEONARD, A. & PEPIN F. 1994 Boundary Conditions for Viscous Vortex Methods. *J. of Comp. Phys.* **113,** 52-61.

KOUMOUTSAKOS, P. 1995 Fast multipole expansion schemes for N-body problems. *Annual Research Briefs.* Center for Turbulence Research, NASA Ames/Stanford Univ., 377-390.

MAS-GALLIC, S. 1987 Contribution à l' analyse numérique des méthodes particulaires. *Thèse d'Etat.* Université Paris VI.

RATHANASINGHAM, R. ,PIEPSZ, O.,GOLDBERG, H. D., SCHMIDT, M., & BREUER, K. S.

994 Performance of sensors and actuators for turbulent flow control. *Bulletin of the American Physical Society.* **39,** 1909.

SADDOUGHI, S. G. 1994 Experimental investigations of "on-demand" vortex generators. *Annual Research Briefs.* Center for Turbulence Research, NASA Ames/Stanford Univ., 197-203.